Proceedings of the ASME 2024
International Design Engineering Technical Conferences and
Computers and Information in Engineering Conference
IDETC-CIE2024
August 25-28, 2024, Washington, DC

DETC2024-143874

EFFECTS OF HIGH FREQUENCY HORIZONTAL BASE EXCITATION ON A BISTABLE SYSTEM

Pritam Ghoshal[1], James M. Gibert[1,*], Anil K. Bajaj[2]

[1]Advanced Dynamics and Mechanics Lab, Ray W. Herrick Laboratories, School of Mechanical Engineering, Purdue University, West Lafayette, Indiana
[2]Ray W. Herrick Laboratories, School of Mechanical Engineering, Purdue University, West Lafayette, Indiana

ABSTRACT

High frequency excitation (HFE) is known to induce various nontrivial effects, such as system stiffening, biasing, and the smoothing of discontinuities in dynamical systems. These effects become increasingly pertinent in multi-stable systems, where the system's bias towards a certain equilibrium state can depend heavily on the combination of forcing parameters, leading to stability in some scenarios and instability in others. In this initial investigation, our objective is to pinpoint the specific parameter ranges in which the bistable system demonstrates typical HFE effects, both through numerical simulations and experimental observations. To accomplish this, we utilize the method of multiple scales to analyze the interplay among different time scales. The equation of slow dynamics reveals how the excitation parameters lead to a change in stability of equilibrium points. Additionally, we delineate the parameter ranges where stabilizing previously unstable equilibrium configurations is achievable. We demonstrate the typical positional biasing effect of high-frequency excitation that leads to a shift in the equilibrium points as the excitation parameter is varied. This kind of excitation can enable the active shaping of potential wells. Finally, we qualitatively validate our numerical findings through experimental testing using a simplistic model made with LEGOs.

Keywords: Biasing, Bifurcation, Bistability, High Frequency Excitation, Multiple Scales, von Mises truss

1. INTRODUCTION

The study of multi-stable systems is slowly gaining traction because of its wide applications in metamaterials and vibration attenuation. Typically these systems have several stable configurations, hence the name multi-stable. One may draw an analogy with several commonplace objects like an electric switch, a hair-clip or a Venus Flytrap. The configuration attained by this kind of system depends on the initial perturbation provided. In this study, we shall focus on a bistable system, that is, it has two stable configurations and an unstable configuration. We represent this class of systems in the form of a von Mises truss (see Figure 1a). Although in reality the system could manifest in any form, for example, a dome-shaped structure or an initially curved beam, we choose to model it using the truss because it simplifies the analysis and also captures the important dynamical behavior of these systems. Prior research on the stability and equilibrium paths of a von Mises truss can be found in [1–3].

The bistable truss under consideration undergoes the phenomenon of snap through, in which the system rapidly transitions from one equilibrium to another under a progressively increasing load. This phenomenon has been studied extensively for elastic systems in [4–8]. Introduction of damping, whether in the form of simple viscous damping or viscoelastic damping, brings in additional layers of complexity in the system. Alhadidi and Gibert [9] showed that a proper tuning of the Deborah number in the viscoelastic system can allow us to control the duration of snap-through. Gomez et al. [10] studied the snap through buckling of a viscoelastic von Mises truss and presented an analytical expression for the snap through time. The delayed snap-through behavior has been studied for both perfect and imperfect shallow truss/arches in [11, 12]. The snap-through dynamics in the presence of viscoelasticity has been exploited in [13, 14].

The dynamic behavior of the von Mises truss in the presence of external excitation is even more interesting [15]. The presence of chaos in such externally excited system has been demonstrated in [16]. The system can exhibit both small and large amplitude motion and even exhibit potential well escapes. Suire and Cederbaum [17, 18] studied the dynamics of viscoelastic bars subjected to harmonic forcing using numerical techniques and demonstrated the presence of chaos. Pourtakdoust and Fazelzadeh [19] studied viscoelastic panel flutter in a supersonic flow. The chaotic behavior in a double beam system was studied by Fang et al

*Corresponding author: jgibert@purdue.edu

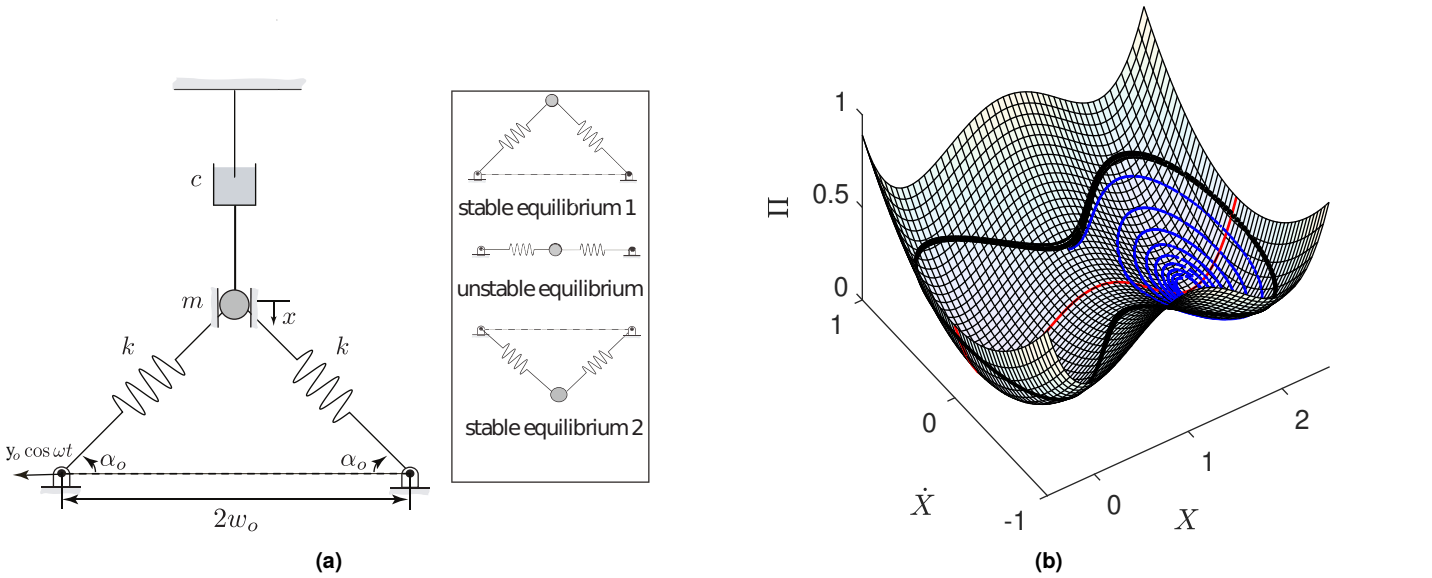

FIGURE 1: (a) Elastic von Mises truss with viscous dashpot. Inset shows the stable and unstable equilibrium configurations. (b) Total energy curve of the unforced system. The red line represents a total energy curve for a given velocity $\dot{X}$, which is symmetric about the saddle point. The black line represents a high energy trajectory with $\zeta = 0$. The blue curve represents a decaying trajectory with $\zeta = 0.05$.

[20]. In addition, researchers [21, 22] studied the effects of parameter changes on the inter-well and intra-well dynamics of a bistable piezoelectric inertial generator and demonstrated the phenomenon of escape from a potential well. Zhou et al. [23] studied the dynamics of tristable energy harvesters and the effect of asymmetric potential wells on the performance of the harvester. The approximate condition for escape from a potential well using the harmonic balance technique was determined by Virgin et al. [24]. Orlando et al. [25] studied the permanent and transient escape in an elastic von Mises truss and the influence of noise on dynamic buckling load.

Under normal circumstances, the von Mises truss will not show any oscillations about the unstable equilibrium. Although adjustments to system parameters can influence snapping behavior (refer to Figure 2), they will not induce oscillations around the unstable equilibrium. Even when the system is harmonically excited, it can only exhibit large-amplitude oscillations about the unstable equilibrium. Stable low-amplitude solutions are not possible in this case because it does not lead to any changes in the effective stiffness in the system.

The question then arises: why do we seek to stabilize the unstable equilibrium? This interest stems from the fact that a bistable system can exist in three states: a natural state, an inverted state, and an unstable state. These discrete states can be visualized as 1 (stable or 'active' states) and 0 (unstable or 'parked' state). Representing states discretely enables tuning excitation parameters to extract oscillations about a desired state. This capability finds broad applications in the realm of mechanical logic gates.

Stabilization of an unstable equilibrium using fast excitation was demonstrated by Kapitza [26] in the context of an inverted pendulum. This paper extends the analytical framework by introducing high-frequency base excitation to bistable systems. While this kind of high-frequency excitation can exhibit trivial behavior, that is, high frequency oscillations about some stable equilibrium configuration, it can also show several non-trivial behavior. The prominent effects of such high frequency excitation have been demonstrated in some revolutionary papers by Thomsen and Tcherniak [27–29]. Typical effects of such high frequency excitation include stiffening [30], biasing [31] and smoothing of discontinuities, for example in stick-slip dynamics [32, 33], symmetry breaking bifurcations [34] and limit cycles [35, 36]. The analysis conventionally involves partitioning slow and fast motions, where the average effect of fast excitation leads to a fictitious force known as the vibrational force [37]. Experimentally, this behavior has been shown to lead to vibrational resonance as a type of nonlinear behavior observed in a bistable system when it experiences a biharmonic force, made up of a small-scale resonant force and a larger, high-frequency force. In certain situations, this high-frequency force enhances the resonant reaction related to the system's slow-moving dynamics [38]. Recently [39] has introduced a method for actively altering the potential energy function of a bistable oscillator without relying on feedback control, which is advantageous for creating adaptive structures, switches, vibration absorbers, and energy harvesters. By nonlinearly coupling the bistable oscillator to a stiff linear oscillator that is harmonically excited near its resonant frequency, the study demonstrates that active control over the oscillator's potential energy function is possible through adjustments in the magnitude and/or frequency of the high-frequency input, facilitating significant changes in shape with relatively low levels of excitation.

In this paper we study the effects of horizontal high frequency excitation on the dynamic behavior of a von Mises truss. We demonstrate how the unstable equilibrium can be stabilized for certain combination of excitation parameters. The method of multiple scales, specifically the direct separation of solutions on

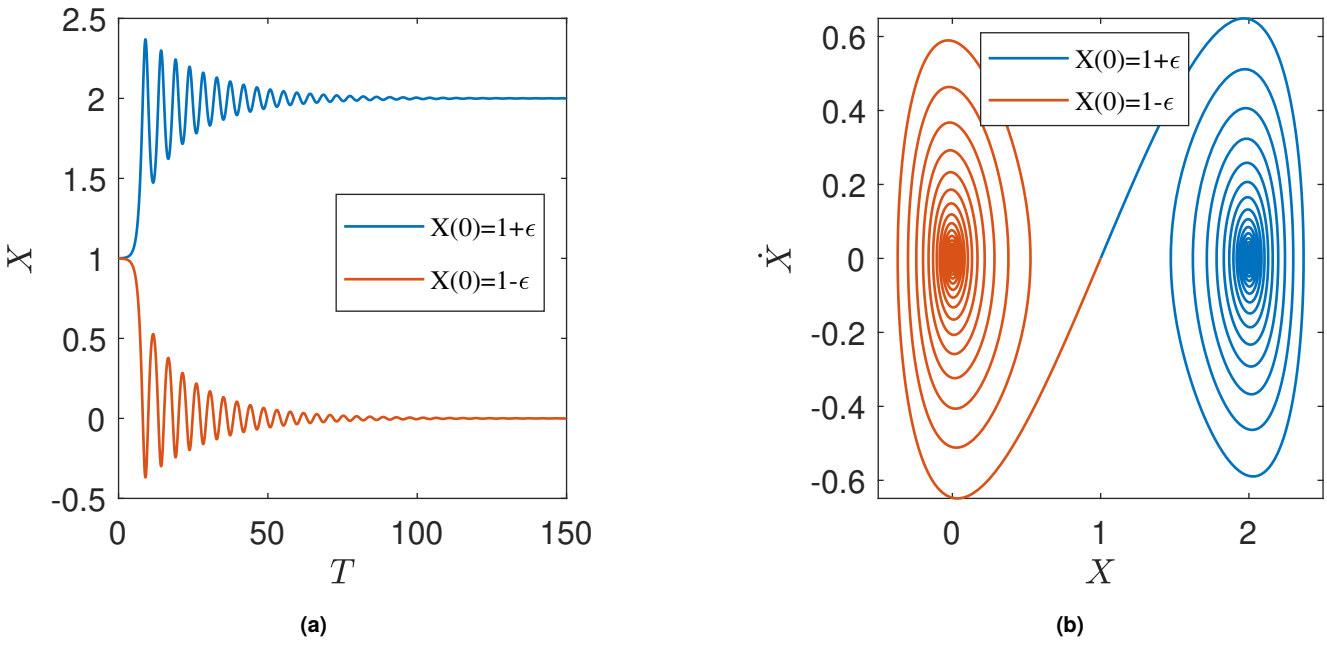

FIGURE 2: Time response and their corresponding phase portrait when the unforced system is released from rest from the unstable equilibrium. The system gets attracted to the potential well towards which it is biased, without any oscillations about the unstable equilibrium.

slow and fast timescales, is employed to capture these intricate dynamical behaviors.

2. MODEL DESCRIPTION

Figure 1a shows the undeformed configuration of the system. At this instant, all springs are unstretched. The tilted springs have a stiffness of k and are inclined at an angle α_0 to the horizontal in the undeformed configuration. The width of the truss is $2w_0$. The entire mass of the system is concentrated at a single point and is equal to m. The mass is connected to a dashpot of viscosity c and is constrained to move in a slot in the vertical direction only, thus eliminating the need to introduce an additional horizontal degree of freedom.

Let the mass be indented downward by an amount x as shown in Figure 1a. At the same instant, the pin joint on the left moves by an amount y (for simplicity, the time dependence of $x(t)$ and $y(t)$ has been dropped from the notation). Assuming the small-angle approximations, the change in length of the two tilted springs are given as

$$\begin{aligned} dl_1 &= \frac{y^2}{2w_0} + y + \frac{x^2}{2w_0} - \alpha_0 x, \\ dl_2 &= \frac{x^2}{2w_0} - \alpha_0 x, \end{aligned} \tag{1}$$

where the subscript 1 and 2 denote the spring which is being excited and the fixed spring respectively. The instantaneous angles made by the springs with the horizontal are given by

$$\begin{aligned} \alpha_1 &= \frac{w_0\alpha_0 - x}{w_0 + y} \approx \frac{w_0\alpha_0 - x}{w_0}, \\ \alpha_2 &= \frac{w_0\alpha_0 - x}{w_0}. \end{aligned} \tag{2}$$

Here we have assumed that the amplitude of the horizontal excitation is much less than the width of the truss and retained only one term in the Taylor series expansion.

Thus the governing equation for the mass is given as

$$m\frac{d^2x}{dt^2} = kdl_1\alpha_1 + kdl_2\alpha_2 - c\frac{dx}{dt}. \tag{3}$$

The horizontal components of the spring forces are balanced by the normal forces on the slot.

3. NON-DIMENSIONALIZATION

We first re-scale time with respect to the timescale of elastic oscillations. Thus, we have $t = \alpha_0^{-1}\sqrt{\frac{m}{k}}T$. The displacements are scaled with respect to the initial height of the truss in the undeformed configuration. Thus we have $x = \alpha_0 w_0 X$ and $y_0 = \alpha_0 w_0 Y_0$. Additionally we have

$$\Omega = \frac{\omega}{\omega_n}, \qquad \zeta = \frac{c}{2m\omega_n}, \tag{4}$$

where ω_n is the natural frequency of oscillations. Note that the restriction of the excitation amplitude being less than the width of the truss enforces a limit on the parameter Y_0. We must have $Y_0 < 1/\alpha_0$.

The governing equation of motion is hence given by

$$\frac{d^2X}{dT^2} + 2\zeta\frac{dX}{dT} + X^3 - 3X^2 + \left(\frac{Y_0^2}{2}\cos^2\Omega T + \frac{Y_0}{\alpha_0}\cos\Omega T + 2\right)X - \frac{Y_0^2}{2}\cos^2\Omega T - \frac{Y_0}{\alpha_0}\cos\Omega T = 0. \tag{5}$$

The equilibrium points of the unforced system ($Y_0 = 0$) are given by $X = 0, 1, 2$, with $X = 0$ being the natural stable configuration,

$X = 2$ being the inverted stable configuration, and $X = 1$ being the unstable configuration in between (when both springs are horizontal).

We consider that the truss is initially indented by applying an instantaneous displacement of X_{ind}. The indentation force is then removed and the base is excited immediately and our external clock is started, i.e., we define $T = 0$ at the time the indenter is released and the base is excited.

The initial conditions for the system are hence given by

$$X(0^+) = X_{\text{ind}}, \quad \dot{X}(0^+) = 0. \tag{6}$$

In this paper, unless otherwise specified, we take $X_{\text{ind}} = 2$.

4. METHOD OF MULTIPLE SCALES

Since the excitation frequency is much larger as compared to the natural frequency of the system, we will decompose the response as a function of two time-scales: a slow time scale of elastic oscillations and a fast time scale corresponding to the external forcing frequency. Let the slow time scale be denoted by $\tau_1 = T$ and the fast time scale be denoted by $\tau_2 = \Omega T$. In terms of these new time-scales our equations of motion become

$$\frac{d^2X}{d\tau_1^2} + 2\zeta\frac{dX}{d\tau_1} + X^3 - 3X^2 + \left(\frac{Y_0^2}{2}\cos^2\tau_2 + \frac{Y_0}{\alpha_0}\cos\tau_2 + 2\right)X - \frac{Y_0^2}{2}\cos^2\tau_2 - \frac{Y_0}{\alpha_0}\cos\tau_2 = 0. \tag{7}$$

We consider that $\Omega \sim \mathcal{O}(\epsilon^{-1})$ where ϵ is a small parameter. Using the method of direct separation of motion into slow and fast components, we assume a solution of the form

$$X(T) = z(\tau_1) + \frac{1}{\Omega^2}\phi(\tau_1, \tau_2) = z(\tau_1) + \epsilon^2\phi(\tau_1, \tau_2). \tag{8}$$

Note that $\mathcal{O}(\epsilon)$ terms have been neglected. This is a consequence of the multiple-scale approach itself and has been directly omitted here to make the calculations simple.

The derivatives are calculated as

$$\frac{d(.)}{dT} = \frac{\partial(.)}{\partial\tau_1} + \frac{1}{\epsilon}\frac{\partial(.)}{\partial\tau_2}. \tag{9}$$

Substituting Equations (8) and (9) in Equation (7) and collecting like powers of ϵ together, we have

$$\ddot{z} + \phi'' + 2\zeta\dot{z} + z^3 - 3z^2 + \left(2 + \frac{Y_0}{\alpha_0}\cos\tau_2 + \frac{Y_0^2}{2}\cos^2\tau_2\right)z - \frac{Y_0}{\alpha_0}\cos\tau_2 - \frac{Y_0^2}{2}\cos^2\tau_2 + \epsilon\left(2\zeta\phi' + 2\dot{\phi}'\right) + \epsilon^2\left(\ddot{\phi} + 2\zeta\dot{\phi} + 2\phi + 3\phi z^2 - 6\phi z + \frac{Y_0}{\alpha_0}\phi\cos\tau_2 + \frac{Y_0^2}{2}\phi\cos^2\tau_2\right) + \mathcal{O}(\epsilon^4) = 0. \tag{10}$$

Here, the dot represents derivatives with respect to τ_1 and dash represents derivatives with respect to τ_2.

Averaging Equation (10) over the fast time scale we obtain

$$\ddot{z} + 2\zeta\dot{z} + z^3 - 3z^2 + \left(2 + \frac{Y_0^2}{4}\right)z - \frac{Y_0^2}{4} + \epsilon^2\left(\frac{Y_0}{\alpha_0} < \phi\cos\tau_2 > + \frac{Y_0^2}{2} < \phi\cos^2\tau_2 >\right) + \mathcal{O}(\epsilon^4) = 0, \tag{11}$$

where $< . >$ denotes the average over the fast time scale. Note that $< \phi >= 0$ and $< z^n >= z^n$. Now subtracting Equations (11) from (10), and considering only the leading order terms, we obtain

$$\phi'' + \frac{Y_0}{\alpha_0}(z-1)\cos\tau_2 + \frac{Y_0^2}{4}(z-1)\cos 2\tau_2 = 0. \tag{12}$$

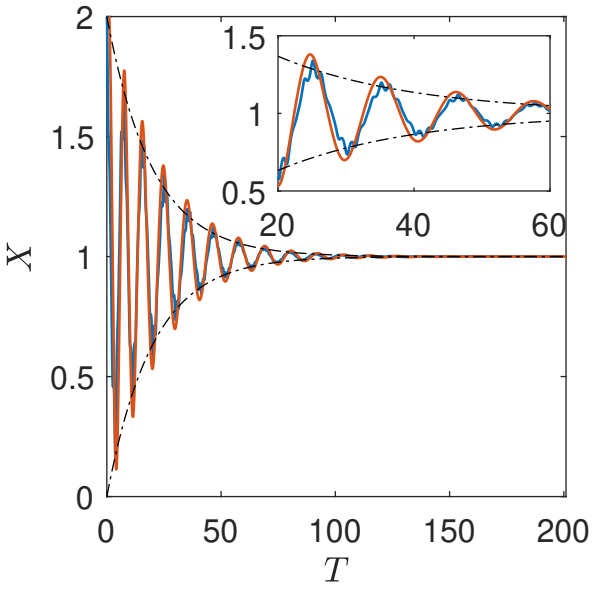

FIGURE 3: Time response of the system under fast excitation for $\alpha_0 = 30°$, $Y_0 = 2$, $\Omega = 5$ and $\zeta = 0.05$.

Equation (12) is an ordinary second order differential equation in ϕ and can be solved exactly. We thus obtain

$$\phi = \frac{Y_0}{\alpha_0}(z-1)\cos\tau_2 + \frac{Y_0^2}{16}(z-1)\cos 2\tau_2. \tag{13}$$

Here we have enforced the condition that there must be no secular terms and that ϕ must average out on the fast time scale τ_2. Equation (13) determines the fast oscillations. Now substituting ϕ in Equation (11) , keeping terms only up to $\mathcal{O}(\epsilon^2)$, back substituting $\epsilon = \Omega^{-1}$, we obtain the equation for the slow dynamics as

$$\ddot{z} + 2\zeta\dot{z} + z^3 - 3z^2 + \left(2 + \frac{Y_0^2}{4} + \frac{Y_0^2}{128\Omega^2} + \frac{Y_0^2}{2\alpha_0^2\Omega^2}\right)z - \left(\frac{Y_0^2}{4} + \frac{Y_0^2}{2\alpha_0^2\Omega^2} + \frac{Y_0^4}{128\Omega^2}\right) = 0. \tag{14}$$

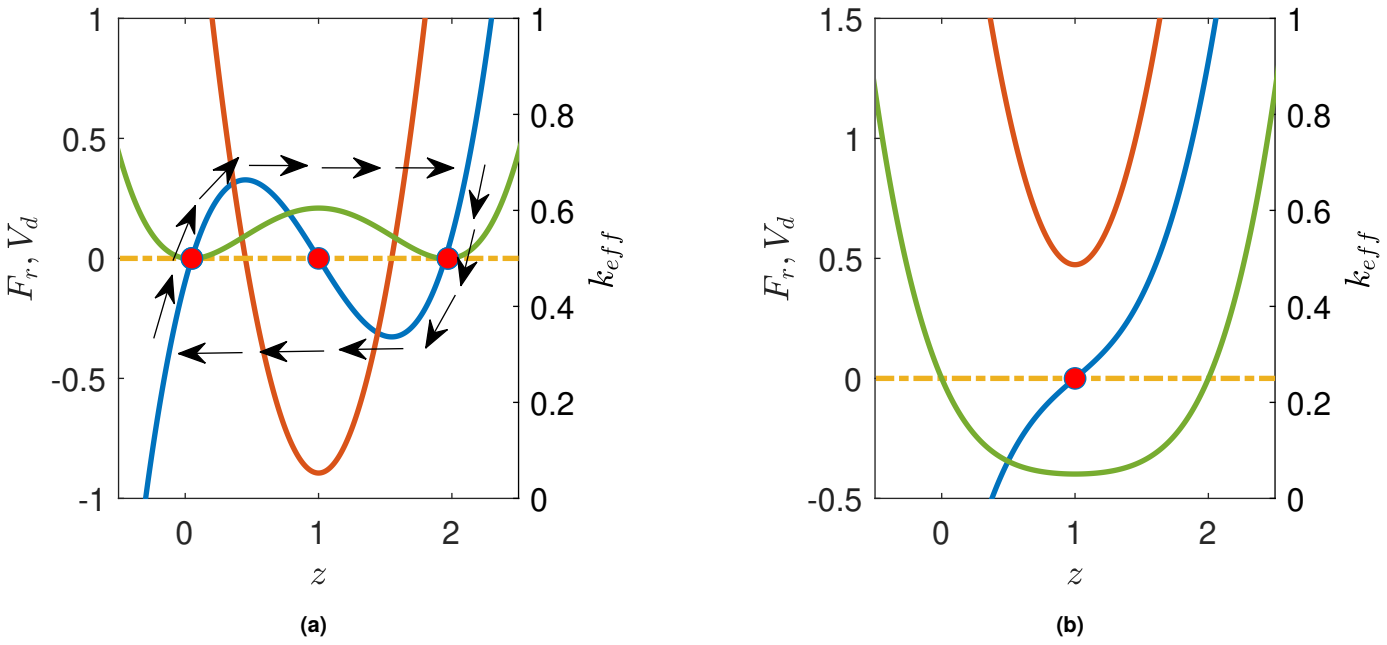

FIGURE 4: Restoring force, effective stiffness and dynamic potential for $\alpha_0 = 30^\circ$, $\Omega = 5$ and (a) $Y_0 = 0.5$ (b) $Y_0 = 2$. Blue curve represents restoring force. Zero crossings represent equilibrium points. Red curves represent effective stiffness. Green curves represent dynamic potential.

Note that the correction terms are directly proportional to Y_0 and inversely proportional to Ω^2. The time response of the system is shown in Figure 3. The blue curve represents the response obtained from numerical simulation. It can be seen that the system now exhibits small amplitude oscillations about the unstable equilibrium configuration which has now been stabilized.

5. THE SLOW EFFECTS OF FAST EXCITATION

In this section, we shall talk about the non-trivial effects of high frequency excitation. The dynamic potential energy of the system (V_d) is given by

$$V_d = \frac{z^4}{4} - z^3 + \left(2 + \frac{Y_0^2}{4} + \frac{Y_0^2}{128\Omega^2} + \frac{Y_0^2}{2\alpha_0^2\Omega^2}\right)\frac{z^2}{2} - \left(\frac{Y_0^2}{4} + \frac{Y_0^2}{2\alpha_0^2\Omega^2} + \frac{Y_0^4}{128\Omega^2}\right)z. \quad (15)$$

Substituting $Y_0 = 0$ gives the static potential (V_s) of the system. Now, when the excitation amplitude is increased, the system transitions from a two-well potential to a single-well potential. The nonlinear restoring force is given by

$$F_r = \frac{dV_d}{dz} = z^3 - 3z^2 + \left(2 + \frac{Y_0^2}{4} + \frac{Y_0^4}{128\Omega^2} + \frac{Y_0^2}{2\alpha_0^2\Omega^2}\right)z - \left(\frac{Y_0^2}{4} + \frac{Y_0^2}{2\alpha_0^2\Omega^2} - \frac{Y_0^4}{128\Omega^2}\right). \quad (16)$$

The effective stiffness (which now depends on the excitation parameters) is given by

$$k_{eff} = \frac{dF_r}{dz} = 3z^2 - 6z + 2 + \frac{Y_0^2}{4} + \frac{Y_0^4}{128\Omega^2} + \frac{Y_0^2}{2\alpha_0^2\Omega^2}. \quad (17)$$

Figure 4 shows the averaged restoring force, the effective stiffness, and the dynamic potential of the system. For $Y_0 = 0.5$, we can see that there are three equilibrium points (points where the restoring force curve crosses the zero line/extremes of the dynamic potential). The corresponding value of stiffness at the equilibrium points determines the stability of the equilibrium. For the two stable equilibrium positions, we have positive stiffness, while for the unstable equilibrium, we obtain negative stiffness. If the truss is indented quasi-statically, it undergoes snap through at the point where the stiffness becomes zero. If the direction of the quasi-static displacement is now reversed, it once again snaps back to its original configuration. However, the path followed is not the same, and this leads to hysteresis. As the excitation amplitude increases, there is a shift in the equilibrium positions. These new equilibrium positions are termed as 'quasi-equilibria'. The quasi-equilibrium positions are given by

$$z_{eq} = 1, 1 \pm \sqrt{1 - \frac{Y_0^2}{4} - \frac{Y_0^4}{128\Omega^2} - \frac{Y_0^2}{2\alpha_0^2\Omega^2}}. \quad (18)$$

These new equilibria are characterized by a higher stiffness value, and hence a larger natural frequency of oscillation. For $Y_0 = 2$, we obtain only a single equilibrium that is stable as indicated by the positive value of the stiffness in Figure 4b. At this point, the two stable equilibria on either side of the unstable equilibrium have coalesced, and the unstable equilibrium has

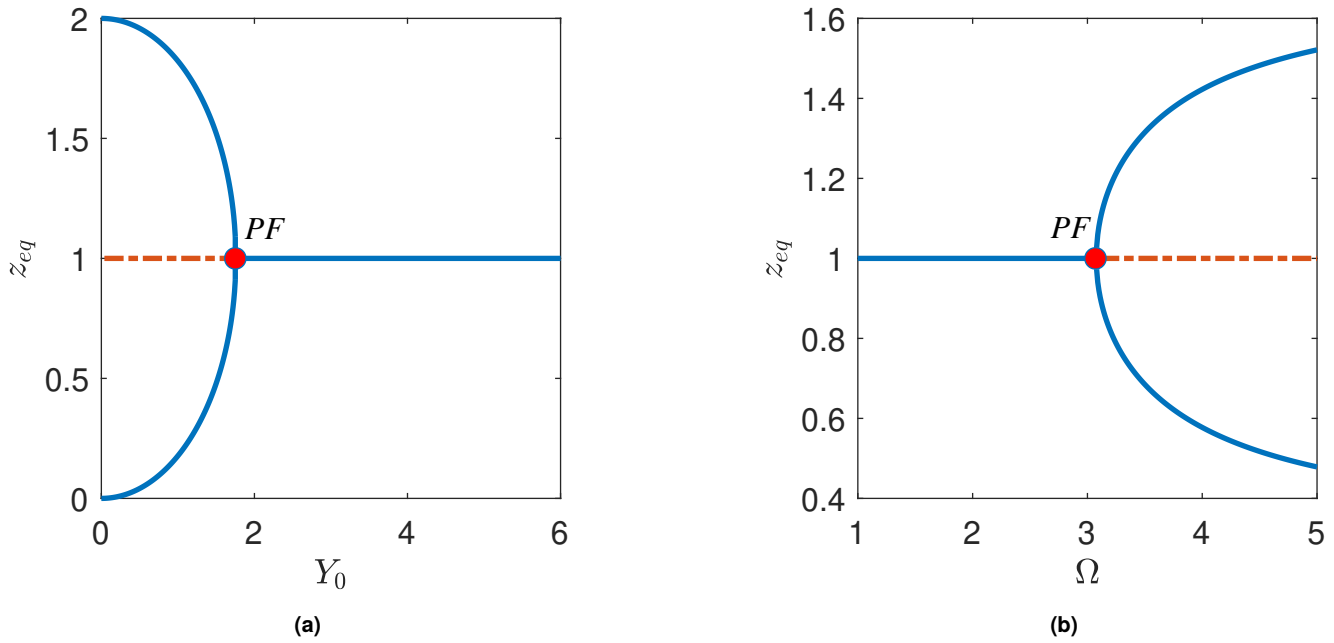

FIGURE 5: Variation of quasi-equilibrium positions for $\alpha = 30^\circ$ with (a) excitation amplitude Y_0 for $\Omega = 5$ (b) excitation frequency Ω for $Y_0 = 1.5$.

disappeared, thus suggesting that a pitchfork bifurcation might have taken place.

The quasi-equilibrium positions have been plotted as a function of Y_0 in Figure 5a. We observe that when $Y_0 = 0$, the steady state equation gives the usual equilibrium points of the unforced system at $z_{eq} = 0, 1, 2$. As the excitation amplitude is increased, we obtain a shift in the stable equilibria. This shift is termed as positional biasing. Beyond a critical value, the unstable equilibrium at $z_{eq} = 1$ becomes stabilized through a supercritical pitchfork bifurcation. For the parameter value chosen ($\alpha_0 = 30^\circ, \Omega = 5$), this threshold turns out to be $Y_{0_{cr}} \approx 1.758$.

It can be seen from Equation (18), that if $Y_0 \geq 2$, then $z_{eq} = 1$ is the only stable equilibrium. On the other hand, for $Y_0 < 2$, depending on the choice of Ω, one may have one or three quasi-equilibria, thus suggesting a pitchfork bifurcation. The bifurcation diagram with respect to Ω is shown in Figure 5b for $Y_0 = 1.5$. It can be seen that a supercritical pitchfork bifurcation destabilizes the stabilized equilibrium.

Although the equilibrium at $z_{eq} = 1$ can be stabilized for certain combinations of excitation amplitude and excitation frequency, the system is still capable of exhibiting both large and small amplitude oscillations about the 'stabilized' equilibrium. Figures 6 and 7 show that parameter space of forcing amplitude and forcing frequency for $\alpha_0 = 30^\circ$ and $\alpha_0 = 5^\circ$ respectively where stabilization is possible and also identify the parameter regimes where the system exhibits small and large amplitude oscillations. The red stars indicate the parameter combinations at which our experimental model has been validated.

The small amplitude oscillations about the unstable equilibrium are of particular interest to us in the context of mechanical logic gates. For a particular combination of excitation parameters, the system can be parked temporarily in the unstable state

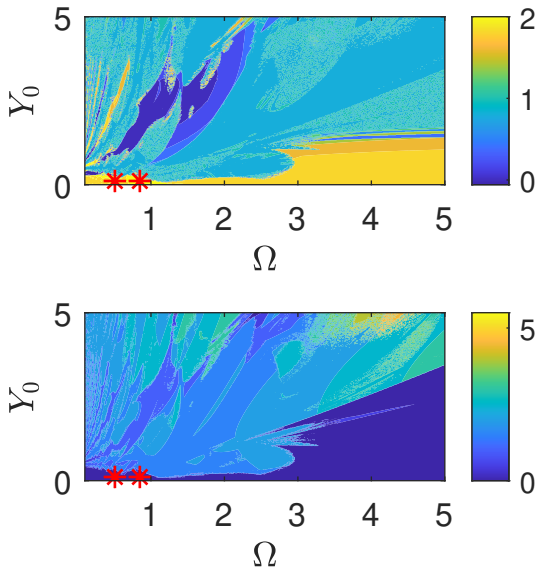

FIGURE 6: Mean (top) and amplitude (bottom) of excitation in the space of excitation amplitude and excitation frequency for $\alpha = 30^\circ$. Red star indicates parameter value chosen for experimental verification ($\Omega = 0.5091$, $Y_0 = 0.111$ and $\Omega = 0.848$, $Y_0 = 0.111$).

allowing no transmission (in an electrical circuit this would correspond to having no electrical contact). An external disturbance to the system may then bias it to one of the stable state, thus allowing transmission (analogous to establishing electrical contact that allows flow of current) as shown in Figure 8.

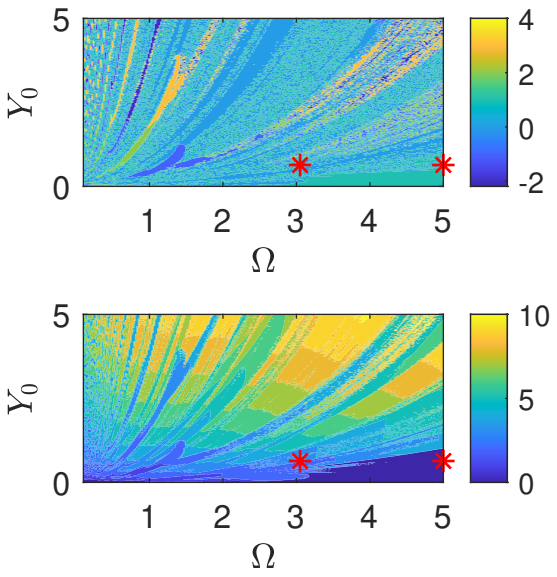

FIGURE 7: Mean (top) and amplitude (bottom) of excitation in the space of excitation amplitude and excitation frequency for $\alpha = 5°$. Red star indicates parameter value chosen for experimental verification ($\Omega = 3.05$, $Y_0 = 0.637$ and $\Omega = 5.092$, $Y_0 = 0.637$).

6. EXPERIMENTAL VALIDATION

The numerical simulations have been qualitatively validated using a straightforward experimental model constructed with LEGO components. The setup comprises a set of three springs, two of which are in parallel to each other, connected at an angle through a pin joint (two springs in parallel are used to avoid any bending at the pin-joint, but their net effective stiffness adds up to the stiffness of the spring on the other side). The springs in parallel are fixed to the shaker at the other end, while the third spring has its end fixed. The setup is shown in Figure 9.

6.1 Procedure

To ensure a proper comparison of the experimental and numerical models, the springs were subjected to a compression test. Within the operational range, the springs exhibit predominantly linear behavior with minimal hysteresis, yielding a spring constant of approximately 1000 N/m for each side. Furthermore, each spring weighs approximately $2g$.

The amplitude of excitation and frequency of excitation are constrained by the maximum power that can be delivered to/from the amplifier and also by the stiffness of the LEGOs. For our purposes, we have fixed the excitation amplitude at $y_0 = 0.1$ in and the excitation frequency at $\omega = 30$ Hz and $\omega = 50$ Hz. The vibrations are tracked using a Chronos high-speed camera at a frame rate of 10488 fps and a resolution of 640×240. The images are then fed into a video tracking software to get the position versus time data. A FFT of the displacement data reveals the dominant frequency component in the response. These frequency components are used to fit a periodic solution to the experimental data. Details of the system parameters used in the experiment and the corresponding outcomes are given in Table 1.

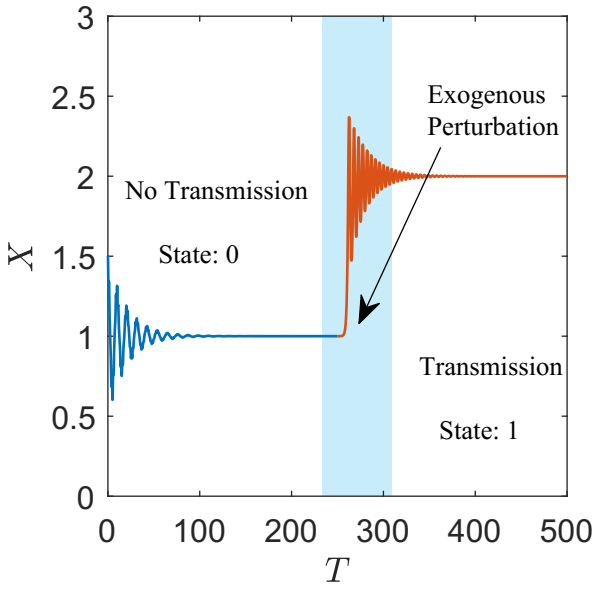

FIGURE 8: The system temporarily parked in the unstable state allowing no transmission. An exogenous perturbation biases it to one of the stable state allowing transmission to occur.

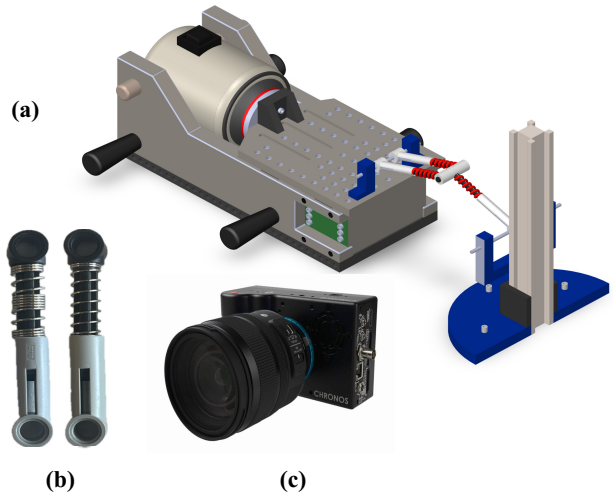

FIGURE 9: (a) Experimental Setup (b) LEGO springs (lego.com) (c) Chronos High-Speed Camera (krontech.ca)

6.2 Observations

For $\alpha_0 = 30°$, it can be seen that the excitation amplitude is below the critical threshold for the parameter values chosen. The truss simply exhibits trivial low amplitude oscillations about the inverted configuration. This can be clearly seen from the phase portraits in Figure 11. On the other hand, for $\alpha = 5°$, the excitation amplitude is above the required threshold for the parameters chosen. Hence in this case we obtain oscillations about the now stabilized unstable equilibrium. These oscillations are of large amplitude for the parameter values chosen.

Figure 12 shows the response of the system for $\omega = 50$ Hz. It can be seen that for $\alpha = 30°$, the system oscillates about the stable equilibria only. A large perturbation causes the system to snap from one equilibrium to the other. For $\alpha = 5°$, the system remains

TABLE 1: System and Excitation Parameters and Outcome

Experiment	α_0 [degree]	y_0 [inch]	ω [Hz]	Threshold Y_0	Supplied Y_0	Outcome
Run 1	30	0.1	30	0.371	0.111	No Stabilization
Run 2	30	0.1	50	0.600	0.111	No Stabilization
Run 3	5	0.1	30	0.371	0.637	Stabilization (large amplitude)
Run 4	5	0.1	50	0.600	0.637	Stabilization (small amplitude)

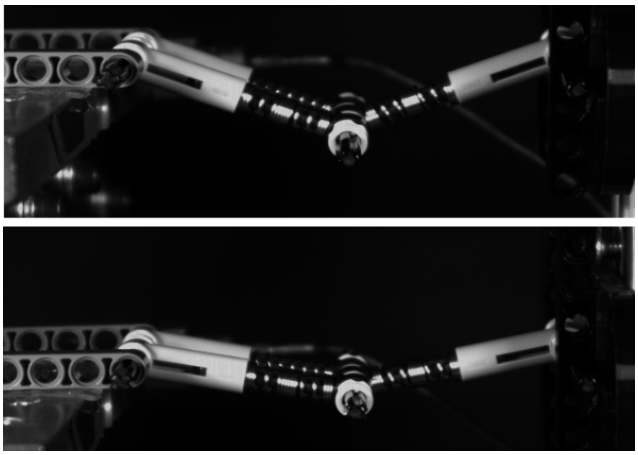

FIGURE 10: Two tested configurations captured using a high speed camera. Top figure corresponds to Run 1 and 2. Bottom figure corresponds to Run 3 and 4.

stabilized in the unstable configuration until a large perturbation causes it go to a large orbit motion.

6.3 Sources of Error

Although the LEGOs offer a simplistic representation of our model, there are potential pitfalls in using them to validate numerical results. Firstly, our numerical model does not account for the horizontal component of oscillations of the mass that take place in the absence of the slot (which has not been implemented in the experimental model). Secondly, the LEGOs themselves lead to flexural and torsional instability in the model, which perturb the system from oscillating around the unstable equilibrium, especially at high frequencies where these modes get excited. Third, the damping in the model is not purely viscous. Ideally, our numerical model should have some linear/nonlinear frictional damping.

7. CONCLUSIONS

In this paper, we studied the effects of high frequency excitation on the stability of a bistable system represented as a von Mises truss. We used the method of multiple scales to study the evolution of the slow dynamics. Specifically, we used the method of direct separation of solutions, which involves writing the solution as a superposition of fast oscillations on the slow dynamics. We demonstrated two primary effects of the fast excitation, stiffening in which the natural frequency of the corresponding equilibrium increases and biasing (more specifically positional biasing) in which the equilibrium point itself changes as the excitation amplitude is varied. Parameter regimes have been identified where stabilization of the unstable equilibrium is possible which has also been validated through a simplistic experimental model.

ACKNOWLEDGMENTS

The authors would like to acknowledge the financial support provided by NSF CAREER Award: CMMI 2145803.

REFERENCES

[1] Pelliciari, Matteo and Tarantino, Angelo Marcello. "Equilibrium paths for von Mises trusses in finite elasticity." *Journal of Elasticity* Vol. 138 No. 2 (2020): pp. 145–168.

[2] Kala, Zdeněk and Kalina, Martin. "Static equilibrium states of von mises trusses." *International Journal of Mechanics* Vol. 10 (2016): pp. 294–298.

[3] Ghoshal, Pritam, Zhao, Qianyu, Gibert, James M. and Bajaj, Anil K. "Effect of Boundary Conditions on the Stability of a Viscoelastic Von Mises Truss." Lacarbonara, Walter (ed.). *Advances in Nonlinear Dynamics, Volume I*: pp. 217–227. 2024. Springer Nature Switzerland, Cham.

[4] Liu, Mingchao, Gomez, Michael and Vella, Dominic. "Delayed bifurcation in elastic snap-through instabilities." *Journal of the Mechanics and Physics of Solids* Vol. 151 (2021): p. 104386.

[5] Falope, Federico Oyedeji, Pelliciari, Matteo, Lanzoni, Luca and Tarantino, Angelo Marcello. "Snap-through and Eulerian buckling of the bi-stable von Mises truss in nonlinear elasticity: A theoretical, numerical and experimental investigation." *International Journal of Non-Linear Mechanics* Vol. 134 (2021): p. 103739.

[6] Fonseca, Filipe Meirelles and Gonçalves, Paulo Batista. "Nonlinear behavior and instabilities of a hyperelastic von Mises truss." *International Journal of Non-Linear Mechanics* Vol. 142 (2022): p. 103964.

[7] Orlando, Diego, de Castro, Carlos Henrique L and Gonçalves, Paulo B. "Nonlinear vibrations and instability of a bistable shallow reticulated truss." *Nonlinear Dynamics* Vol. 94 (2018): pp. 1479–1499.

[8] Virgin, LN. "On the elastic snapping of structural elements." *International Journal of Non-Linear Mechanics* Vol. 149 (2023): p. 104329.

[9] Alhadidi, Ali H and Gibert, James M. "A new perspective on static bifurcations in the presence of viscoelasticity." *Nonlinear Dynamics* Vol. 103 No. 2 (2021): pp. 1345–1363.

[10] Gomez, Michael, Moulton, Derek E and Vella, Dominic. "Dynamics of viscoelastic snap-through." *Journal of the Mechanics and Physics of Solids* Vol. 124 (2019): pp. 781–813.

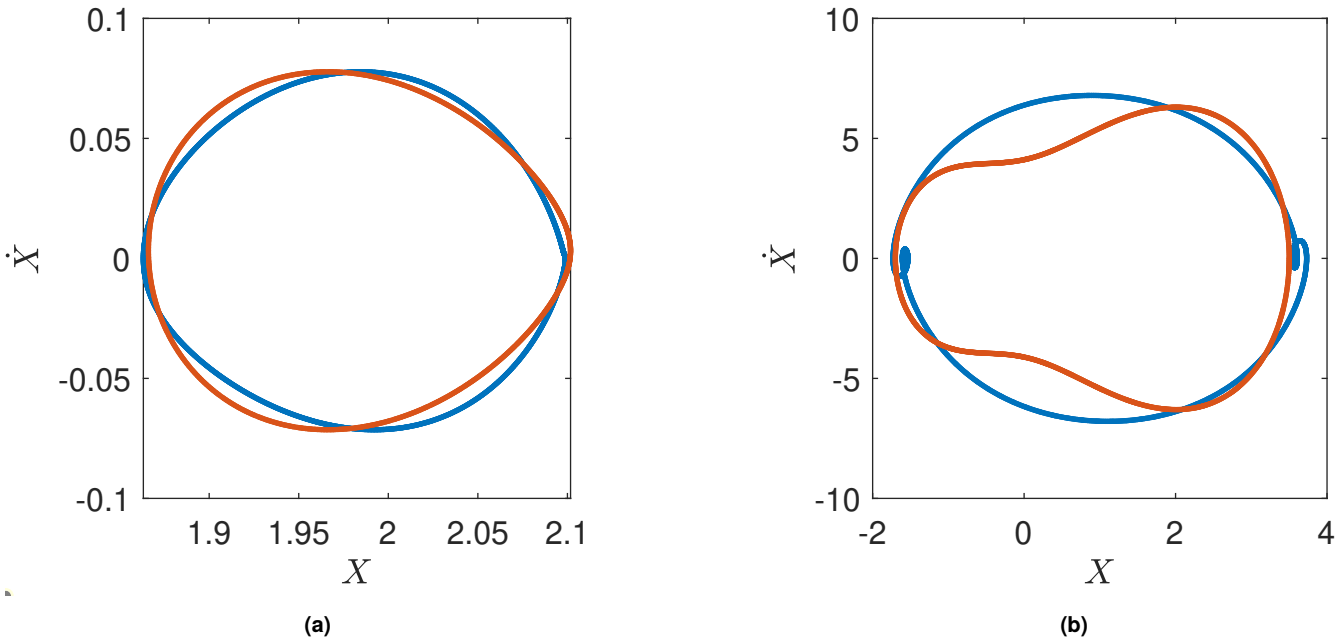

FIGURE 11: Comparison of experimental and numerical phase portraits. Blue curve corresponds to numerical simulation. Red curve corresponds to experimental model. (a) Small amplitude oscillations about the stable equilibrium (b) Large amplitude oscillations about stabilized equilibrium.

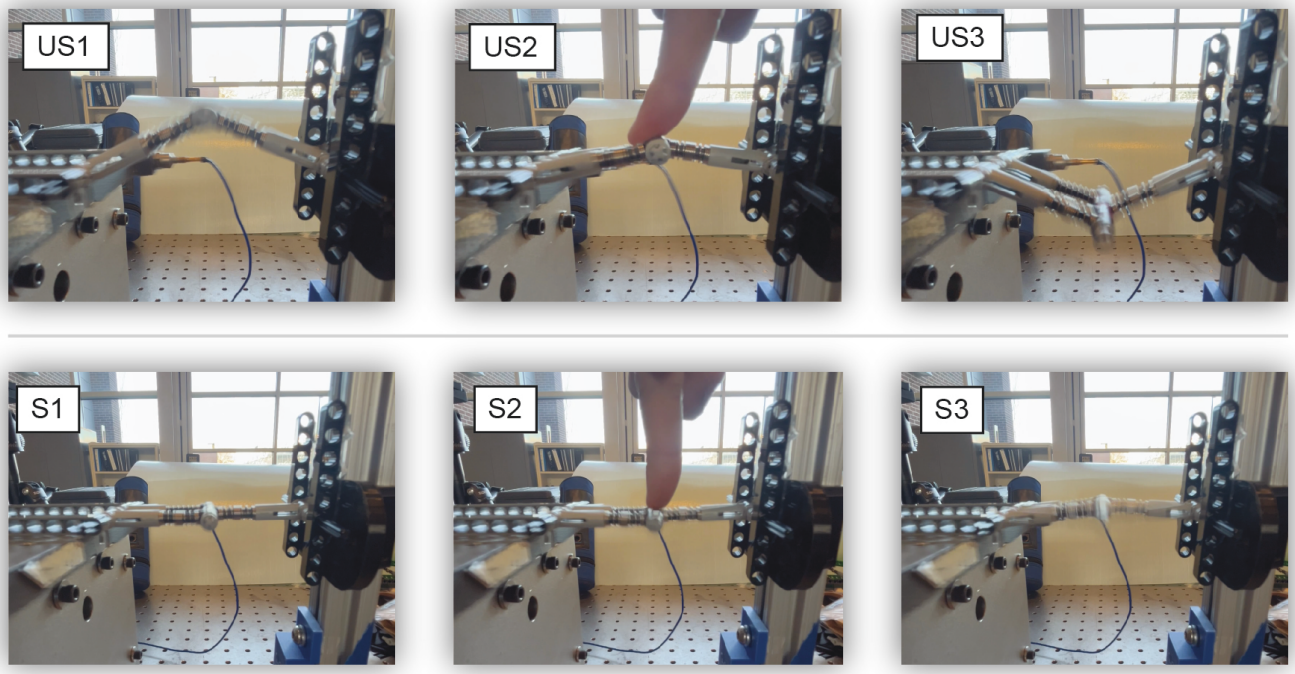

FIGURE 12: Frequency Stabilized equilibrium points: Top row US 1-3 indicates equilibrium points at $\omega = 50$ Hz, $\alpha_0 = 30°$. US1 indicates oscillation about the natural equilibrium point. US2 is a perturbation disturbance caused by depressing the center point of the system, and US3 is oscillation about the inverted equilibrium point. Bottom row S 1-3 indicates frequency stabilized equilibrium points at $\omega = 50$ Hz, $\alpha_0 = 5°$. S1 indicates oscillation about stabilized equilibrium point, S2 indicates perturbation disturbance caused by depressing the center point of the system, and S3 show return to stabilized equilibrium point.

[11] Huang, N. C. and Nachbar, W. "Dynamic Snap-Through of Imperfect Viscoelastic Shallow Arches." *Journal of Applied Mechanics* Vol. 35 No. 2 (1968): pp. 289–296. DOI 10.1115/1.3601194.

[12] Nachbar, W and Huang, NC. "Dynamic snap-through of a simple viscoelastic truss." *Quarterly of Applied Mathematics* Vol. 25 No. 1 (1967): pp. 65–82.

[13] Dykstra, David MJ, Busink, Joris, Ennis, Bernard and Coulais, Corentin. "Viscoelastic snapping metamaterials." *Journal of Applied Mechanics* Vol. 86 No. 11 (2019): p. 111012.

[14] Dykstra, David M. J., Janbaz, Shahram and Coulais, Corentin. "The extreme mechanics of viscoelastic metamaterials." *APL Materials* Vol. 10 No. 8 (2022): p. 080702. DOI 10.1063/5.0094224.

[15] Ghoshal, Pritam, Gibert, James M. and Bajaj, Anil K. "Periodic Response and Stability Analysis of a Bistable Viscoelastic Von Mises Truss." Preprint available at SSRN: https://ssrn.com/abstract=4730137.

[16] Ghoshal, Pritam, Gibert, James M. and Bajaj, Anil K. "The Presence of Chaos in a Viscoelastic Harmonically Forced Von Mises Truss." *Journal of Computational and Nonlinear Dynamics* Vol. 19 No. 7 (2024): p. 071009. DOI 10.1115/1.4064554.

[17] Suire, Guillaume and Cederbaum, Gabriel. "Elastica type dynamic stability analysis of viscoelastic columns." *Archive of Applied Mechanics* Vol. 64 No. 5 (1994): pp. 307–316.

[18] Suire, Guillaume and Cederbaum, Gabriel. "Periodic and chaotic behavior of viscoelastic nonlinear (elastica) bars under harmonic excitations." *International journal of mechanical sciences* Vol. 37 No. 7 (1995): pp. 753–772.

[19] Pourtakdoust, SH and Fazelzadeh, SA. "Chaotic analysis of nonlinear viscoelastic panel flutter in supersonic flow." *Nonlinear Dynamics* Vol. 32 (2003): pp. 387–404.

[20] Fang, Hui, Liu, Ze and Duan, Liya. "Enhanced dissipation in a double-beam system with a bistable constraint." *Archive of Applied Mechanics* Vol. 92 No. 3 (2022): pp. 885–901.

[21] Stanton, Samuel C, McGehee, Clark C and Mann, Brian P. "Nonlinear dynamics for broadband energy harvesting: Investigation of a bistable piezoelectric inertial generator." *Physica D: Nonlinear Phenomena* Vol. 239 No. 10 (2010): pp. 640–653.

[22] Stanton, Samuel C, Owens, Benjamin AM and Mann, Brian P. "Harmonic balance analysis of the bistable piezoelectric inertial generator." *Journal of Sound and Vibration* Vol. 331 No. 15 (2012): pp. 3617–3627.

[23] Zhou, Shengxi and Zuo, Lei. "Nonlinear dynamic analysis of asymmetric tristable energy harvesters for enhanced energy harvesting." *Communications in Nonlinear Science and Numerical Simulation* Vol. 61 (2018): pp. 271–284.

[24] Virgin, Lawrence N, Plaut, Raymond H and Cheng, Ching-Chuan. "Prediction of escape from a potential well under harmonic excitation." *International Journal of Non-linear Mechanics* Vol. 27 No. 3 (1992): pp. 357–365.

[25] Orlando, Diego, Gonçalves, Paulo B, Lenci, Stefano and Rega, Giuseppe. "Influence of the mechanics of escape on the instability of von Mises truss and its control." *Procedia Engineering* Vol. 199 (2017): pp. 778–783.

[26] Kapitza, Peter Leonidovich. "A pendulum with oscillating suspension." *Uspekhi fizicheskikh nauk* Vol. 44 (1951): pp. 7–20.

[27] Thomsen, Jon Juel. "Some general effects of strong high-frequency excitation: stiffening, biasing and smoothening." *Journal of Sound and Vibration* Vol. 253 No. 4 (2002): pp. 807–831.

[28] Tcherniak, Dmitri and Thomsen, Jon Juel. "Slow effects of fast harmonic excitation for elastic structures." *Nonlinear Dynamics* Vol. 17 (1998): pp. 227–246.

[29] Tcherniak, Dimitri. "The influence of fast excitation on a continuous system." *Journal of sound and vibration* Vol. 227 No. 2 (1999): pp. 343–360.

[30] Jensen, Jakob Søndergaard, Tcherniak, DM and Thomsen, Jon Juel. "Stiffening effects of high-frequency excitation: experiments for an axially loaded beam." *J. Appl. Mech.* Vol. 67 No. 2 (2000): pp. 397–402.

[31] Hansen, Morten Hartvig. "Effect of high-frequency excitation on natural frequencies of spinning discs." *Journal of sound and vibration* Vol. 234 No. 4 (2000): pp. 577–589.

[32] Thomsen, Jon Juel. "Using fast vibrations to quench friction-induced oscillations." *Journal of sound and vibration* Vol. 228 No. 5 (1999): pp. 1079–1102.

[33] Thomsen, Jon Juel and Fidlin, Alexander. "Analytical approximations for stick–slip vibration amplitudes." *International Journal of Non-Linear Mechanics* Vol. 38 No. 3 (2003): pp. 389–403.

[34] Mann, BP and Koplow, MA. "Symmetry breaking bifurcations of a parametrically excited pendulum." *Nonlinear Dynamics* Vol. 46 (2006): pp. 427–437.

[35] Belhaq, Mohamed and Sah, Si Mohamed. "Horizontal fast excitation in delayed van der Pol oscillator." *Communications in Nonlinear Science and Numerical Simulation* Vol. 13 No. 8 (2008): pp. 1706–1713.

[36] Sah, Simohamed and Belhaq, Mohamed. "Effect of vertical high-frequency parametric excitation on self-excited motion in a delayed van der Pol oscillator." *Chaos, Solitons & Fractals* Vol. 37 No. 5 (2008): pp. 1489–1496.

[37] Blekhman, Iliya I. *Vibrational mechanics: nonlinear dynamic effects, general approach, applications*. World Scientific (2000).

[38] Abusoua, Abdrouf and Daqaq, Mohammed F. "Experimental evidence of vibrational resonance in a mechanical bistable twin-well oscillator." *Journal of Computational and Nonlinear Dynamics* Vol. 13 No. 6 (2018): p. 061002.

[39] Daqaq, Mohammed F. "Active shaping of a bi-stable potential: Exploring nonlinear coupling to a stiff externally-excited oscillator." *Journal of Sound and Vibration* Vol. 566 (2023): p. 117919.